ISSN 1674-1056
http://cpb.iphy.ac.cn
http://iopscience.iop.org/cpb
中国物理 B
Chinese Physics
中国物理
Chinese Physics B

Recent advances in non-Pb-based group-IV chalcogenides for environmentally-friendly thermoelectric materials

Bing-Sheng Du(杜炳生), Ji-Kang Jian(简基康), Hai-Tao Liu(刘海涛), Jiao Liu(刘骄), Lei Qiu(邱磊)
Citation: Chin. Phys. B . 2018, 27(4): 048102. **doi:** 10.1088/1674-1056/27/4/048102

Journal homepage: http://cpb.iphy.ac.cn; http://iopscience.iop.org/cpb

What follows is a list of articles you may be interested in

Germanene nanomeshes:Cooperative effects of degenerate perturbation and uniaxial strain on tuning bandgap

Yan Su(苏燕), Xinyu Fan(范新宇)
Chin. Phys. B . 2017, 26(10): 108101. **doi:** 10.1088/1674-1056/26/10/108101

Geometrically induced π-band splitting in graphene superlattices

Yanpei Wei(魏艳佩), Tiantian Jia(贾甜甜), Gang Chen(陈刚)
Chin. Phys. B . 2017, 26(2): 028103. **doi:** 10.1088/1674-1056/26/2/028103

Tunable thermoelectric properties in bended graphene nanoribbons

Chang-Ning Pan(潘长宁), Jun He(何军), Mao-Fa Fang(方卯发)
Chin. Phys. B . 2016, 25(7): 078102. **doi:** 10.1088/1674-1056/25/7/078102

Improved thermoelectric property of cation-substituted $CaMnO_3$

Pradeep Kumar, Subhash C. Kashyap, Vijay Kumar Sharma, H. C. Gupta
Chin. Phys. B . 2015, 24(9): 098101. **doi:** 10.1088/1674-1056/24/9/098101

Gate-dependent photoresponse in self-assembled graphene p-n junctions

Yin Wei-Hong, Wang Yu-Bing, Han Qin, Yang Xiao-Hong
Chin. Phys. B . 2015, 24(6): 068101. **doi:** 10.1088/1674-1056/24/6/068101

TOPICAL REVIEW — Recent advances in thermoelectric materials and devices

Recent advances in non-Pb-based group-IV chalcogenides for environmentally-friendly thermoelectric materials*

Bing-Sheng Du(杜炳生)[1], Ji-Kang Jian(简基康)[1,†], Hai-Tao Liu(刘海涛)[1,2], Jiao Liu(刘骄)[1], and Lei Qiu(邱磊)[1]

[1] School of Physics and Optoelectronic Engineering, Guangdong University of Technology, Guangzhou 510006, China
[2] School of Physical Science and Technology, Xinjiang University, Urumqi 830046, China

(Received 19 December 2017; revised manuscript received 24 January 2018; published online 10 March 2018)

Pb-based group-IV chalcogenides including PbTe and PbSe have been extensively studied as high performance thermoelectric materials during the past few decades. However, the toxicity of Pb inhibits their applications in vast fields due to the serious harm to the environment. Recently the Pb-free group-IV chalcogenides have become an extensive research subject as promising thermoelectric materials because of their unique thermal and electronic transport properties as well as the enviromentally friendly advantage. This paper briefly summarizes the recent research advances in Sn-, Ge-, and Si-chalcogenides thermoelectrics, showing the unexceptionally high thermoelectric performance in SnSe single crystal, and the significant improvement in thermoelectric performance for those polycrystalline materials by successfully modulating the electronic and thermal transport through using some well-developed strategies including band engineering, nanostructuring and defect engineering. In addition, some important issues for future device applications, including N-type doping and mechanical and chemical stabilities of the new thermoelectrics, are also discussed.

Keywords: non-Pb, thermoelectric, group-IV chalcogenides

PACS: 81.05.Zx, 28.41.Ak **DOI:** 10.1088/1674-1056/27/4/048102

1. Introduction

Thermoelectric (TE) materials, a kind of functional materials able to realize direct energy conversion between heat and electricity, have been extensively studied due to the great desire for clean energy.[1] The dimensionless figure of merit $zT = (S^2\sigma T/\kappa)$ is used to characterize the performance of TE material, where S is the Seebeck coefficient, σ is the electrical conductivity, T is the absolute temperature and κ is the thermal conductivity ($\kappa = \kappa_e + \kappa_l$, κ_e is the electronic thermal conductivity, κ_l is the lattice thermal conductivity). Therefore, the high performance TE material should have a low thermal conductivity (κ) and large S and σ.[2–4] Unfortunately the three parameters, i.e., S, σ, and κ, are strongly coupled, and thus preventing the thermoelectric performance from improving by singularly tuning one of them. In the last few decades, the zT values of thermoelectrics have been constantly improved through the successful utilizations of new concepts and mechanisms including defect engineering,[5] band engineering,[6,7] nanostructuring,[8,9] nanoinclusions,[10,11] and modulation doping.[12,13]

The strategies mentioned above have been applied to many TE material systems, such as Half-Heuslers,[14] Skutterudites,[11] Bi_2Te_3[10,15] and PbTe,[16] making great achievements. Among those material systems, PbTe has been well investigated for a long history, and most important concepts and strategies for enhancing the TE performances were developed or started in PbTe. The high TE performance for PbTe is related to its intrinsic electronic band structure possessing two valence bands (L and Σ) with a small energy offset that can be further reduced by band engineering to obtain a high band degeneracy, resulting in the improved zT.[17] Besides band engineering, defect engineering has also been utilized to tune the phonon transport in PbTe and obtain a high zT value of 2.2 by their synergistic effects.[18] Despite the fact that great achievements have been made in PbTe-based thermoelectrics, that Pb seriously harms the environment is still a fatal weakness that hinders its large-scale applications.

In 2014, SnSe single crystal was found to have an unprecedentedly high zT value of 2.6 along the crystallographic direction b axis, which uncovered and testified the great potential applications in non-Pb based group-IV chalcogenides thermoelectrics,[19] including tin-, germanium-, and silicon-chalcogenides, because they have the same crystal structure as and similar band structures to PbTe and SnSe.[6,20] As seen from Fig. 1, the number of publications related to the non-Pb based group-IV chalcogenides thermoelectrics has been quickly growing since 2013, implying that the increasing attention has been paid to the research field. Besides the surprising discovery in SnSe single crystals, more exciting achievements have been made in those materials more recently, such

*Project supported by the National Natural Science Foundation of China (Grant Nos. 51472052 and U1601213).
†Corresponding author. E-mail: jianjikang@126.com
© 2018 Chinese Physical Society and IOP Publishing Ltd

as the high zT values of 1.6 and 1.4 for SnTe[21] and GeTe-based thermoelectrics,[22] respectively. These studies reveal the possibility that the higher TE performance beyond that of PbTe can be realized in those eco-friendly group-IV chalcogenides although there are still many challenges.

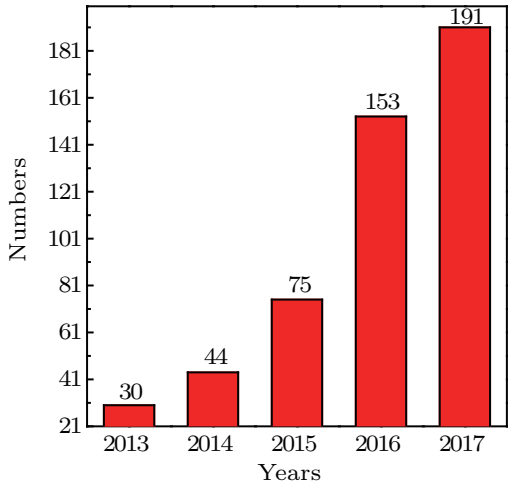


Fig. 1. (color online) Increasing trend of publications relating to non-Pb based group-IV chalcogenide thermoelectrics since the year of 2013. The statistics is performed based on the collection from the Web of Science.

In this paper, we outline the research advances in the group-IV chalcogenides out of PbTe and PbSe in recent years, trying to give a rough guide to this rising topic of thermoelectricity. We first survey the basic crystal and electronic band structural parameters of the materials, showing their potential applications in thermoelectrics. Then we present some typical researches on Sn-, Ge-, and Si-based chalcogenide thermoelectrics, respectively, in which high TE performance has been achieved by utilizing some recently developed strategies or approaches in PbTe thermoelectrics to tune the thermal and electronic transport in those materials. Finally we briefly discuss the possible challenges in the N-type doping, mechanical and chemical stabilities of these TE materials for the future device applications.

2. General considerations of crystal structures and electronic band structures

The crystal structures and electronic band structures of IV-chalcogenides thermoelectrics are briefly summarized in Table 1 and Fig. 2, which can give a basic clue to the speculation of the possible intrinsic thermoelectric properties of the non-Pb based compounds as referenced to Pb-based compounds. It can be seen that SnTe has an NaCl structure with the space group $Fm\bar{3}m$ that is the same as those of PbTe, PbSe, and PbS, and its lattice constants have a just about 2% deviation from those of PbTe. Consequently, SnTe has a similar electronic band structure to that of PbTe, including two valence bands (light band and heavy band), leading to high band degeneracy.[30] At room-temperature, the other IV–VI compounds including SnSe, GeSe, SnS, and GeS all crystallize into GeS-type orthorhombic structure with space group Pnma, and they have similar lattice constants. Such a layered crystal structure contains eight atoms and two adjacent double layers in the primitive cell, which can be regarded as a three-dimensional distortion of the NaCl structure.[20] The electronic structure is another important piece of information to consider the thermoelectric properties of materials. Table 1 presents the band gaps of SnSe, SnTe, SnS, GeSe, GeS, GeTe, SiSe, SiS, and Si_2Te_3, showing that most of the IV-chalcogenides have narrow bandgaps, suggesting their potentials as thermoelectric materials. The calculated band structures of SnS, SnSe, GeS, and GeSe are shown in Fig. 2, revealing that they are indirect semiconductors except GeSe. In Figs. 2(b) and 2(d), the sharp peaks appear near valence band maxima and conduction band minima in the densities of states of SnS and GeS monolayers, which may enhance the Seebeck coefficient.[29]

Table 1. Crystal structures and band gaps of IV-chalcogenide thermoelectrics.

Crystal	Space group	a/Å	b/Å	c/Å	Vol/Å^3	Band gap/eV	Reference
PbTe	$Fm\bar{3}m$	6.46	6.46	6.46	269.50	0.30	[18]
PbSe	$Fm\bar{3}m$	6.12	6.12	6.12	229.70	0.29	[23]
PbS	$Fm\bar{3}m$	5.94	5.94	5.94	209.20	0.42	[23]
SnTe	$Fm\bar{3}m$	6.33	6.33	6.33	253.30	0.18	[21]
SnSe	$Pnma$	11.50	4.15	4.44	212.00	0.61	[19]
	$Cmcm$	4.31	11.70	4.31	217.70	0.39	[19]
SnS	$Pnma$	11.19	3.98	4.33	193.00	1.07	[24]
GeTe	$Pnma$	10.95	4.03	4.45	196.40	0.20	[25]
GeSe	$Pnma$	10.82	3.83	4.39	182.10	0.85	[26]
GeS	$Pnma$	10.47	3.64	4.30	163.90	1.25	[20]
SiSe	$Pmma$	6.64	3.98	9.44	249.47	1.22	[27]
SiS	$Pmma$	7.02	4.00	14.98	420.63	1.35	[27]
Si_2Te_3	$P\bar{3}1c$	6.95	6.95	15.17	643.90	1.78	[28]

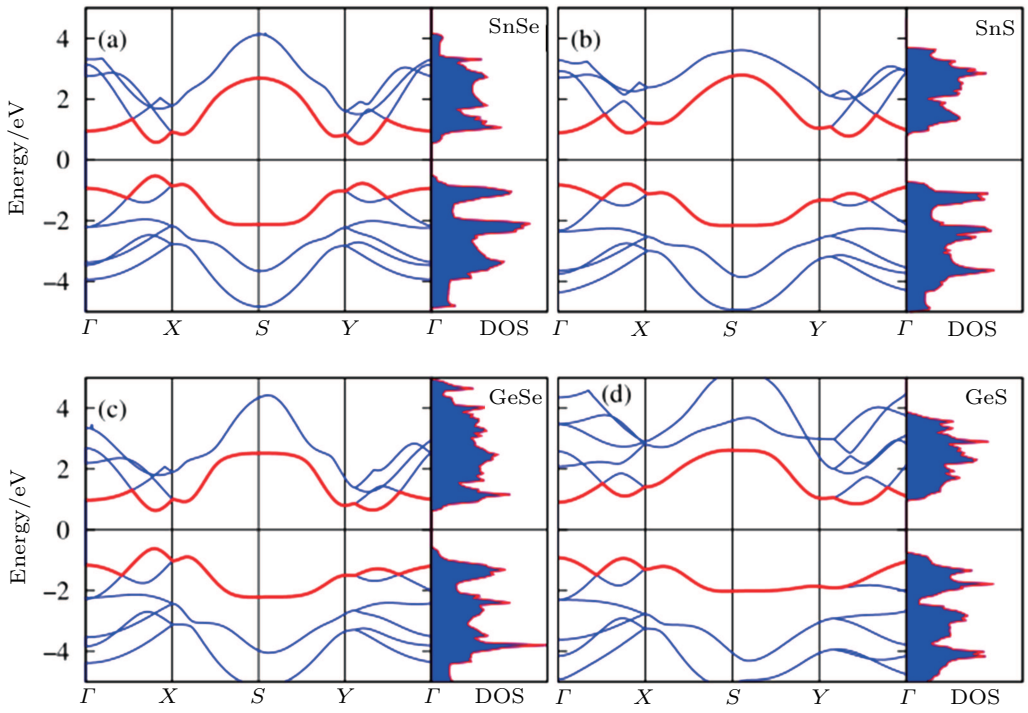


Fig. 2. (color online) Band structures along the high-symmetry k-points Γ, X, S, and Y, and density of states of (a) SnSe, (b) SnS, (c) GeSe, and (d) GeS.[29] (Reprinted from Ref. [29]).

Considering the similarity in the crystalline and electronic band structures of SnTe and PbTe, it is reasonable to anticipate that the high thermoelectric performance can be achieved in SnTe by applying those successful strategies used in PbTe. Meanwhile, the layered structures of those orthorhombic Sn- and Ge-chalcogenides also imply their anisotropic thermoelectric transports, which might lead to their high thermoelectric performances. In the following sections, the detailed discussion is categorized according to the specific material systems that are tin-, germanium- and silicon-chalcogenides, respectively.

3. Tin-chalcogenides (SnSe, SnS, SnTe)

As an alternative analogue of PbTe, SnTe has received more attention from the thermoelectric field due to their high similarity in crystal and electronic band structures. However, an unexceptional breakthrough was first achieved in SnSe. As a narrow band gap semiconductor, SnSe was noticed because of its photo electronic potentials[31,32] instead of thermoelectric properties. The SnSe is an intrinsic P-type material with a carrier concentration in a range of 10^{17} cm^{-3}–10^{18} cm^{-3} and an electrical resistivity between 10^{1} Ω·cm–10^{5} Ω·cm at room temperature.[33] These features make SnSe widely studied and used in solar cells,[34] optoelectronics,[35] and other electronic devices.[36] Recently, the unexceptionally high zT of 2.66±0.3 at 923 K along the b-crystallographic direction was found in un-doped SnSe single crystal, which soon made SnSe a focus of the thermoelectric community.[19] Soon after the first report on un-doped SnSe single crystals,[19] some reports were presented by Zhao *et al.*[37] and Zhou *et al.*,[38] respectively. Na-doped SnSe single crystal with greatly increased hole concentration realized a record-high average zT of $\sim$ 1.34 from 300 K to 773 K[37] and an average zT of $\sim$ 1.2 from 300 K to 800 K,[38] respectively. Inspired by the surprising discovery in SnSe single crystal, some consequent researches on its polycrystalline form were carried out, but the much lower zT of $\sim$ 0.5 was obtained[39] as seen in Fig. 3 that summarizes some reports on thermal conductivity and zT's for SnSe samples with different forms and compositions. To improve zT of SnSe polycrystal, the nanostructuring strategy was implemented.[40,41] Well-crystallized SnSe single crystal nanobelts were prepared by the hydrothermal approach and then were pressed into bulk material by spark plasma sintering.[41] As shown in Fig. 2(a), the lower thermal conductivity was achieved in the nanobelt sample than that in the single-crystal sample, which was considered to be due to the enhanced phonon scattering. The improvement in zT from about 0.5 (SnSe normal polycrystals) to about 0.8 was reported.[41] Introducing some nano-inclusions is another effective approach to reducing the lattice thermal conductivity of the matrix. Recently, some kinds of nanoparticals including PbSe[42,43] and SnTe[44] have been introduced into the SnSe polycrystalline nanocomposites as inclusions and the encouraging results were reported. A high zT value of 1.7 in bulk SnSe polycrystals was obtained by embedding 1% PbSe into the matrix of SnSe nanopowder, and the PbSe secondary phase was found to distribute in the grain boundaries of

SnSe.[42] The nano-inclusions made the electrical conductivity and power factor of the SnSe phase significantly enhanced, resulting in high zT values of 1.7 and 1.4 in parallel and perpendicular to the pressing direction, respectively.[42] Doping is a common approach to increasing the carrier concentration and adjusting the band structure of a material. The thermoelectric properties of Na doped into the P-type SnSe polycrystalline[45] have been reported. It was reported that the heavy P-type doping lowers the Fermi level and increases carrier concentration, leading to a collaborative optimization of the power factor.[12] In addition the point defects enhance the scattering phonons, which reduces the thermal conductivity.[44] The P-type SnSe polycrystal has been prepared by 1% Na doping, which enhanced the carrier concentration and electrical conductivity, meanwhile maintained a relatively large Seebeck coefficient of 142 μV/K and a lower thermal conductivity than the undoped SnSe polycrystal. The 1% Na- doped SnSe shows a maximum zT of ~ 0.8.[45]

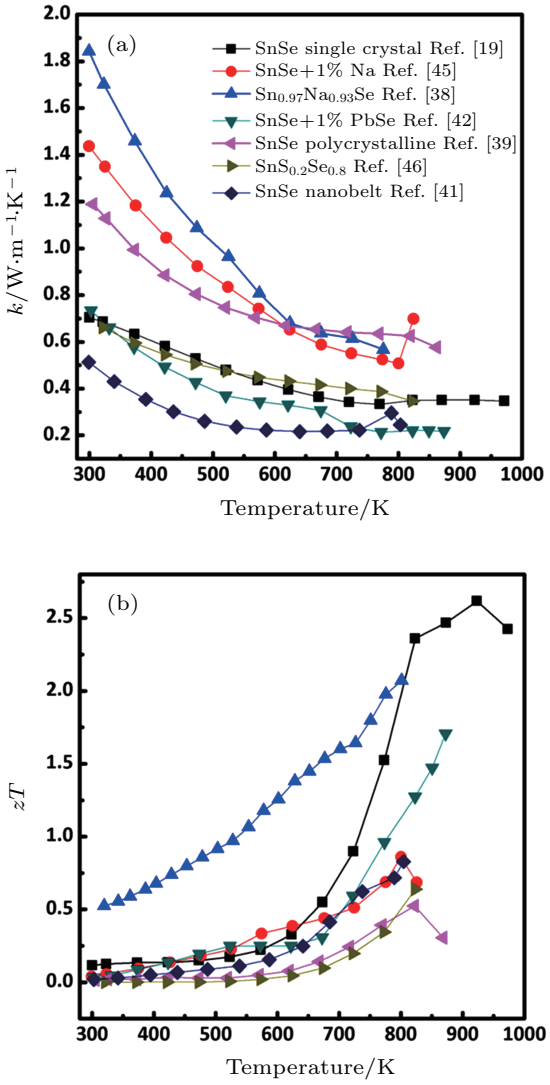


Fig. 3. (color online) Temperature-dependent (a) thermal conductivities and (b) zT values of SnSe single crystal,[19] SnSe+1%Na,[45] $Sn_{0.97}Na_{0.03}Se$,[38] SnSe+1%PbSe,[42] SnSe polycrystalline,[39] $SnS_{0.2}Se_{0.8}$,[46] and SnSe nanobelt.[41]

The SnS has the same crystal structure as that of SnSe at room temperature, and is considered as a promising new thermoelectric material that has an abundant resource and a better environmental compatibility.[47] The pristine SnS shows a high Seebeck coefficient and low thermal conductivity, but the low carrier concentration leads to low electrical conductivity that results in a low zT value. The pristine SnS shows a carrier concentration of about 10^{15} cm^{-3} $\sim$ 10^{17} cm^{-3} and a maximum zT value of 0.16 at 873 K.[48] The P-type SnS was doped with 0.5% Ag bulk material synthesized by a mechanical alloying method, and the derived powders were pressed into pellets by using spark plasma sintering (SPS) and thus improving the zT value from 0.16 to 0.6. The improvement arises from the significantly increased electrical conductivity by Ag doping on Sn sites which greatly increased the carrier concentration ($n_{ave} \approx 10^{18}$ cm^{-3}).[48] The electric conductivity and phonon scattering were also increased simultaneously in $SnS_{0.2}Se_{0.8}$ solid solution, and thus obtaining a high zT of 0.82 at 823 K, which is much higher than that in the pristine SnS compound.[46] Although the significant increase of zT for SnS-based material has not been achieved to date, it is worth further investigating as a potential thermoelectric material.

As shown in Table 1, there are more similarities between SnTe and PbTe including the rock-salt crystal structure, small band gaps, and complex valence band structure,[21] than between SnSe and SnS. However, as summarized in Ref. [17], SnTe has some intrinsic factors that greatly degrade its thermoelectric performance. The SnTe is an intrinsically P-type semiconductor with a high P-type carrier concentration (about 10^{21} cm^{-3}) due to a large number of Sn vacancies in the lattice. Such a high carrier concentration leads to a low Seebeck coefficient and high thermal conductivity, and finally results in low thermoelectric performance in pristine SnTe. In spite of a very high electrical conductivity about $\sim$ 7000 S·cm^{-1} caused by the high carrier concentration, a high total thermal conductivity and a low Seebeck coefficient of about 20 μV·K^{-1} were simultaneously obtained, consequently a low zT value (about 0.2) was achieved at room temperature.[40] However, recent studies have largely improved the thermoelectric performance of SnTe, proving that the SnTe is a promising thermoelectric material through some strategies individually/synergistically applied, which included band engineering,[30] all-scale hierarchical architecturing,[49] defect,[50] and nano-inclusive.[51] Specifically, a record peak zT value of 1.6 in P-type SnTe has been reported by Pei *et al.* via the synergistic effects of the band convergence and interstitial defects.[21] Figure 4 shows the thermoelectric transport data and zT values of SnTe-based thermoelectric,[21] and the data of PbTe-based material[18] are also presented for comparison. The main results presented in the Ref. [21] are briefly depicted as follows, which can clearly show the effectiveness of the band and defect engineering.

The addition of MnTe with sufficiently high concentration into the matrix of SnTe leads to well-converged valence bands and highly enhances the Seebeck coefficient as seen in Fig. 4(a). The enhanced Seebeck coefficient for $Sn_{0.86}Mn_{0.14}Te$ was comparable to that for PbTe at 840 K. It should be noted that the electrical conductivity of $Sn_{0.86}Mn_{0.14}Te$ is lower than that of pristine SnTe due to the decrease of carrier concentration. On the other hand, the addition of MnTe greatly reduces both k_e and k_l by reducing the carrier concentration and enhancing the phonon scatter, finally gives a high zT value of 1.0 that is 2.5 times that of pristine P-type SnTe. To further reduce the k_l for $Sn_{0.86}Mn_{0.14}Te$, the Cu_2Te nano-particles were introduced into the matrix to form interstitial defects at high temperature. It was found that the Seebeck coefficient and resistivity in a broad temperature range were not significantly affected, suggesting that the influence of 5% Cu_2Te on the electronic transport properties was negligible. However, a decrease of the k_l was achieved, giving a record zT value of 1.6 in P-type SnTe, which is four times that of pristine SnTe. The advantages of both band convergence and phonon scattering by interstitial defects realize a high zT value.[21] Besides the band engineering and defects engineering, the nanostructuring strategy was also used in SnTe thermoelectrics. The SnTe nano-particles have been prepared by the hydrothermal approach, and the dramatically reduced thermal conductivity led to a high zT value of 0.79 at 873 K.[39]

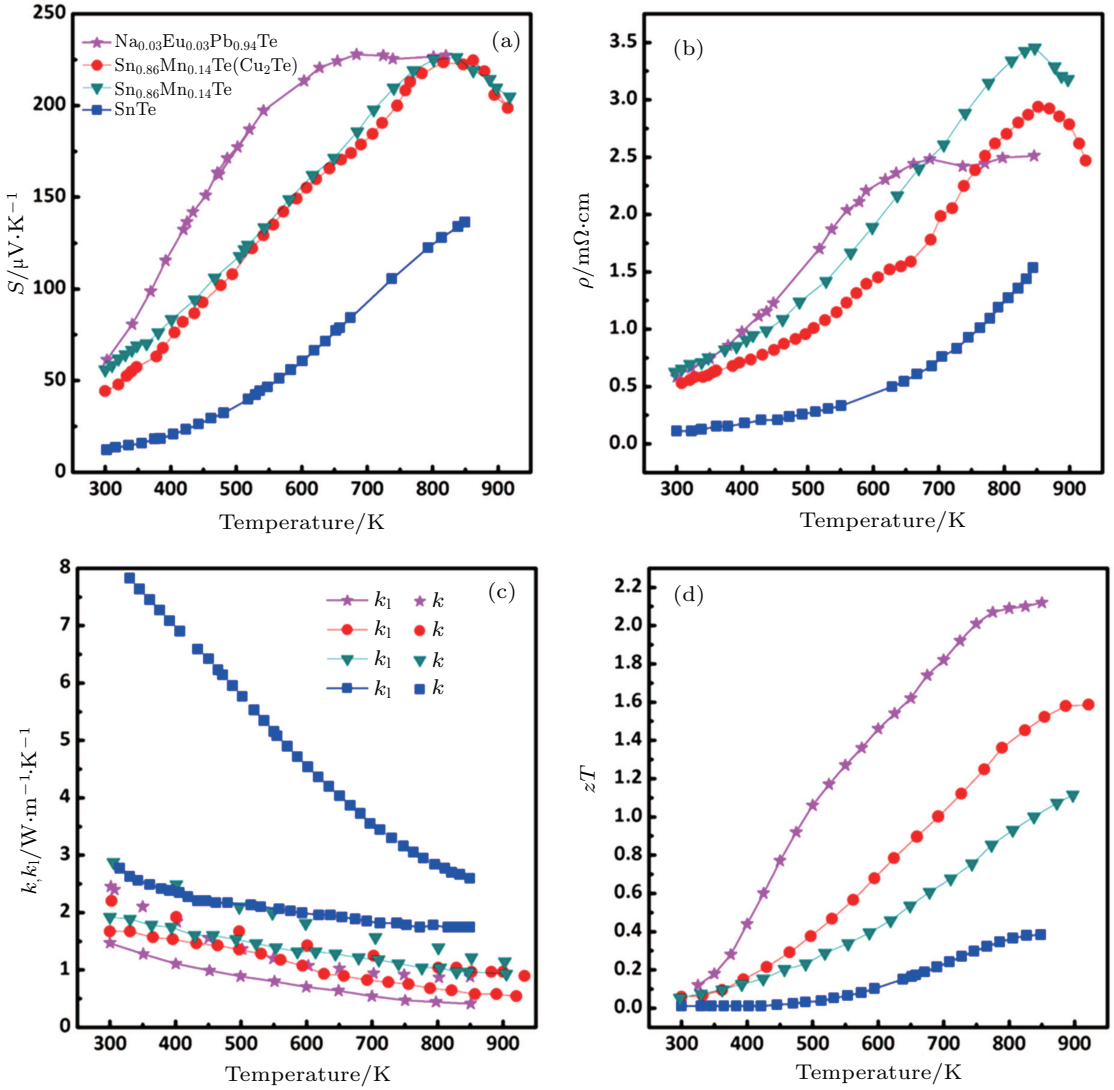


Fig. 4. (color online) Temperature-dependent (a) Seebeck coefficients, (b) resistivities, (c) thermal conductivities, and (d) zT values of the SnTe,[21] $Sn_{0.86}Mn_{0.14}Te$,[21] $Sn_{0.86}Mn_{0.14}Te(Cu_2Te)_{0.05}$,[21] and $Na_{0.03}Eu_{0.03}Pb_{0.94}Te$.[18]

4. Germanium-chalcogenides (GeTe, GeSe, and GeS)

The GeTe-based alloys have been known for a long time for their promising thermoelectric properties due to their superior structural and thermal properties.[52] The GeTe as a P-type semiconductor shows a narrow band gap with a high electrical conductivity and carrier concentration (10^{21} cm^{-3}), which is due to a large number of Ge vacancies.[53] In spite of the high electrical conductivity, the low Seebeck coefficient and high thermal conductivity were also exhibited in the pristine GeTe.

For these reasons, the pristine GeTe exhibited a maximum zT value of 0.88 at 712 K.[54] The doping, band engineering, and nanostructuring have been applied to GeTe for high TE performance. Recently, the GeTe–$AgSbTe_2$-based alloys,[54] Ge–Sb–Te ternary alloys,[25,55] doped GeTe,[56,57] and Ge–Pb–Te alloys[22] each have shown a significant enhancement in zT value as seen in Fig. 5. Some elements such as In,[56] Pb,[22] Sb,[25] and Bi[57] have been doped into the GeTe matrix occupying the site of Ge in the matrix to act as donors to reduce the Ge vacancies, leading to the decrease of hole concentration.

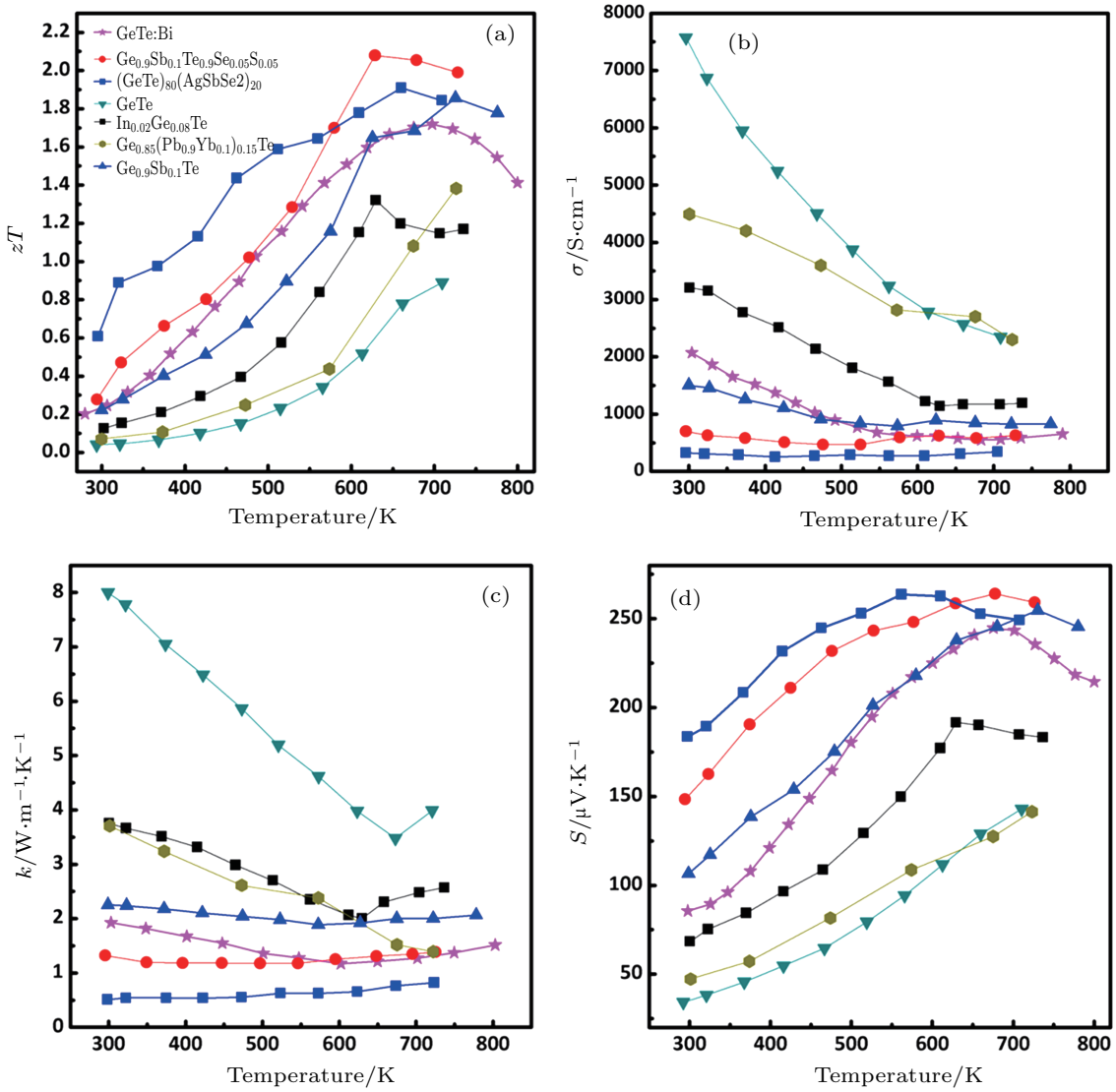


Fig. 5. (color online) Temperature-dependent (a) zT values, (b) conductivities, (c) thermal conductivities, and (d) Seebeck coefficients of GeTe(GeTe,[54] $In_{0.02}Ge_{0.98}Te$,[56] and GeTe:Bi[57]), $(GeTe)_{80}(AgSbSe_2)_{20}$,[54] Ge–Sb–Te alloys ($Ge_{0.9}Sb_{0.1}Te$,[25] and $Ge_{0.9}Sb_{0.1}Te_{0.9}Se_{0.05}S_{0.05}$[55]), and Ge–Pb–Te materials ($Ge_{0.85}(Pb_{0.9}Yb_{0.1})_{0.15}Te$[22]).

It was found that in spite of the decrease of the electrical resistivity, the substitution of 2% In for Ge in GeTe enlarged the Seebeck coefficient, and remarkably reduced the total thermal conductivity, which finally achieved a high zT value of 1.3 at temperature near 628 K in $In_{0.02}Ge_{0.98}Te$.[56] The group-V elements Sb- and Bi-doped GeTe also achieved effective reduction in the carrier concentration and collectively increased the Seebeck coefficient from $\sim 30\ \mu V{\cdot}K^{-1}$ to $\sim 100\ \mu V{\cdot}K^{-1}$, and $\sim 80\ \mu V{\cdot}K^{-1}$.[25,57] Importantly, Sb in GeTe not only reduced the carrier concentration, but also enhanced the valence band degeneracy that highly increased the Seebeck coefficient. Combining with the meso-structured significant decrease in the thermal conductivity, the high thermoelectric figure of merit of 1.85 at 725 K in $Ge_{0.9}Sb_{0.1}Te$[25] was realized. Similarly, Bi in the GeTe matrix also got a zT value of 1.8 at 700 K.[57] The rhombohedral GeTe and rock-salt type $AgSbTe_2$ could form complete solid solution $(Ge–Te)_x(AgSbTe_2)_{100-x}$ (named TAGS).[58] The $AgSbTe_2$ increased density of states of TAGS, and the lead TAGS showed a high Seebeck coefficient.[53] The high thermoelectric figure of merit of 1.5 at 750 K was achieved in TGAS-85.[59] The new pseudo-binary solid solution $(Ge\text{-}Te)_{80}(AgSbSe_2)_{20}$[54] underwent phase-separation and the formation of hierarchical nano/mesostructures, which caused extensive scattering of

heat carrying phonons of different wavelengths, leading to ultra low $k_{lat} \approx 0.4$ W·m^{-1}·K^{-1}, a high peak zT of 1.9 at 660 K, and an ultrahigh average zT of 1.4 in a temperature range of 300K–700 K.[54] The $Ge_{0.9}Sb_{0.1}Te_{0.9}Se_{0.05}S_{0.05}$[55] also exhibited a low κ_{lat} of 0.7 W·m^{-1}·K^{-1} at 730 K due to a broad set of multiple types of mass fluctuations such as Ge/Sb,Te/Se, Te/S, and Se/S that enhanced the phonon scattering. As a result, the SPS-processed $Ge_{0.9}Sb_{0.1}Te_{0.9}Se_{0.05}S_{0.05}$ sample showed a remarkably high zT of 2.1 at 630 K.[55]

The GeSe and GeS have similar crystal structures to SnSe. The orthorhombic layered GeSe and GeS have been predicted as good thermoelectric materials via theoretical calculation,[20] but the experimental investigation indicated that the polycrystalline GeSe with a low carrier concentration showed a low zT value of only 0.2 at 700 K.[60] The elemental doping could be an effective route to optimizing the carrier concentration, but it is still challenging work to ahieve realiable doping experimentally in the GeSe compound.

For these reasons above, the alloying strategy has been used in GeSe by adding the $AgSbSe_2$,[61] which made a structural phase transition from the original orthorhombic structure to a high symmetry rhombohedral phase, and thus obtaining a higher Seebeck coefficient, a modified band structure, and a higher carrier concentration (1.2×10^{20} cm^{-3}). As a result, a zT of 0.86 was achieved. The GeS had a larger band gap (about 1.25 eV) than those of SnSe and GeSe, leading to a low carrier concentration and large Seebeck coefficient. A large power factor of GeS could be obtained by alloying and reasonable doping strategy.[20]

5. Silicon-chalcogenides (SiSe, SiS, Si_2Te_3)

Although SiS and SiSe are of an isostructure with SnSe, they have received less attention than other group-IV chalcogenides up to now. Thermoelectrics properties of SiS and SiSe monolayers have been prdicted via the first-principles calculation as we can see in Fig. 6.[27] The theoretical calculation predicted that SiS (SiSe) can achieve zT values as high as 1.06 (0.92) and 1.99 (1.79) at $T = 500$ K and $T = 700$ K, respectively.[27] The chemical stability of Si-based chalcogenide becomes a problem that maybe inhibits their future applications. In an Si–Te system, the Si_2Te_3 is only stable phase with space group of $P31c$.[62] Using first-principles density functional theory and semiclassical Boltzmann transport theory, the thermoelectric property of Si_2Te_3 has been pridicted, showing that the maxima of zT are 1.86 and 0.34 for N-doped and P-doped materials at 1000 K, respectively.[28] The theoretical studies have revealed the thermoelectric potentials of Si-chalcogenides, but the experimental difficulties, in particular, in synthesizing the materials should be overcome.

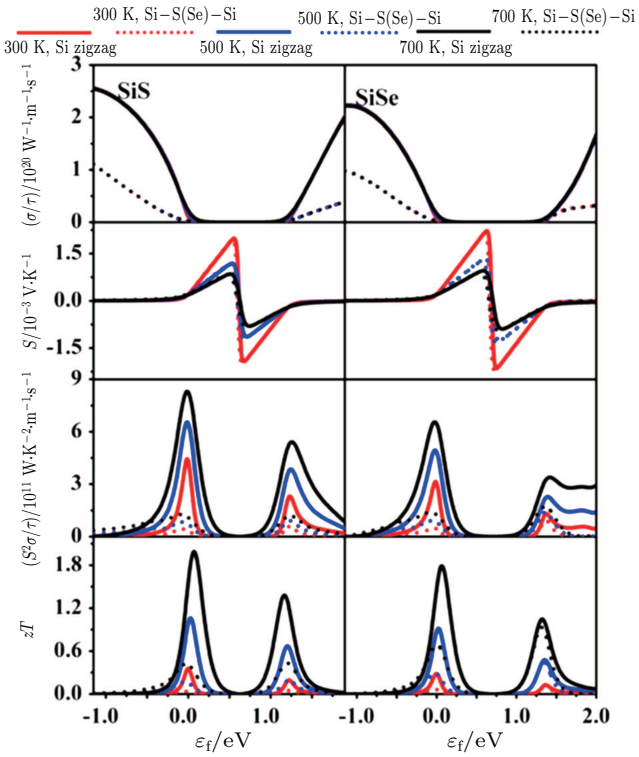


Fig. 6. (color online) [(a) and (e)] Electrical conductivities, [(b) and (f)] Seebeck coefficients, [(c) and (g)] power factors, and [(d) and (h)] zT values of SiS and SiSe each as a function of electron chemical potential ε_f at three different temperatures: $T = 300$, 500, and 700 K and along two anisotropic directions, respectively. Here ε_f refers to the valence band maximum of SiS or SiSe. (Reprinted (adapted) from Ref. [27] with permission from Copyright (2017) American Chemical Society).

6. N-type doping

The above promising results indicate that they are all achieved in P-type materials. It is known that the intrisic metallic ion vacancies in group IV–chalcogenides result in their P-type conductivities and make it difficult to realize reliable N-type doping.[21,51,55] In order to achieve the P–N conduction transition and enhance the electrical conductivity, the effective heavy doping is necessary. However, it is diffcult to realize heavy doping, which is possibly due to the lower solubility of the dopants in group IV–chalcogenide lattices. Some studies demonstrated that extra group- IV metal and halogen elements were promising candidates. Figure 7 summarizes the reported carrier concentrations of some N-type and P-type group-IV chalcogenides. The pristine SnSe,[19,38] SnTe,[51] and GeTe[22] are P-type semiconductors each with a higher hole concentration. There have been some studies carried out to achieve N-type doping in some of those materials, (see the summarized results in Fig. 7(a). But the effective approach to realizing the N-type doping still needs to be explored to optimize the carrier concentation (10^{19}–10^{20}) for thermoeletric applications. There are two kinds of dopants in the IV and VI compounds, which substitute for IV site and VI site, respectively. Some reports showed that Bi, Sb, Pb, and In could substitute for IV site to form N-type conductivity.[63–65,67]

The N-type single crystal SnSe has been achieved by Bi doping, and the carrier concentrations of about 10^{16} cm^{-3} and 2×10^{19} cm^{-3} were obtained at room terperature and 773 K, respectively. Consequently a high zT value of 2.2 at 723 K has been achieved in N-type single crystal.[63] The N-type GeTe has also been achieved by Bi doping.[64] The N-type polycrystalline SnSe has been prepared by Pb and Ti doping, and the $Sn_{0.94-x}Pb_xTi_{0.06}Se$ presents a maxium carrier concentration of 2.64×10^{18} cm^{-3} at room temperature with $x = 0.3$.[66] N-type SnTe by In doping showed a high carrier concentration (4×10^{20} cm^{-3}), in which In not only acted as a hole dopant but also partly filled In5s–Te5p hybridized state centered around Fermi energy E_F.[67] Similarly, the N-type SnTe, GeTe, and SnSe should also be achieved by the above dopants, which needs to be further examined. The VI site is generally substituted by halogens such as Cl, Br, and I to form N-type conductivity. The N-type SnSe was achieved by substituting Br[68]and Cl[69] for Se, and the N-type carrier concentrations were 1.86×10^{19} cm^{-3} and 1.56×10^{19} cm^{-3} at room temperature, and their zT values are 0.54 and 0.6 at 793 K, respectively. Kutorasinski *et al*. performed the calculation based on the density functional theory to compare the valence band and conduction band characteristics of N-type with those of P-type SnSe for the cases where the N- and P-type SnSe have low temperature, middle temperature and high temperature phases, and the results are shown in Fig. 8.[71] It can be found that the Fermi surfaces of N- and P-type SnSe present different features depending on the carrier concentration. For the N-type SnSe semiconductor, when the carrier concentration is

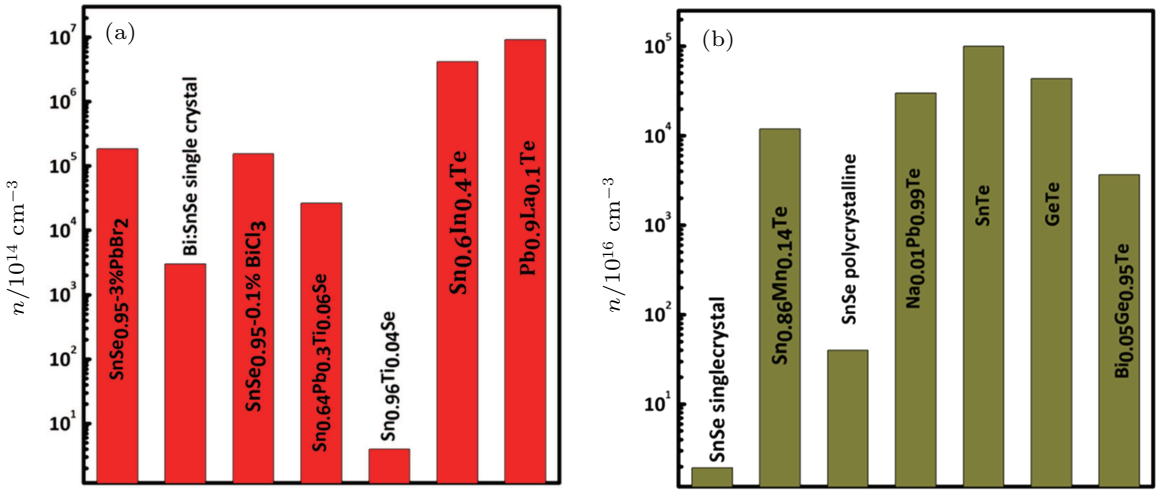


Fig. 7. (color online) (a) N-type carrier concentrations of some doped IV–VI compounds at room temperature: N-type IV–VI compounds ($SnSe_{0.95}$+3%PbBr,[68] Bi:SnSe single crystal,[63] $SnSe_{0.95}$+0.1%$BiCl_3$,[69] $Sn_{0.64}Pb_{0.3}Ti_{0.06}Se$,[66] $Sn_{0.96}Ti_{0.04}Se$,[66] $Sn_{0.6}In_{0.4}Te$,[67] and $Pb_{0.9}La_{0.1}Te$[70]), (b) P-type IV–VI compounds (SnSe single crystal,[19] $Sn_{0.96}Mn_{0.14}Te$,[21] SnSe polycrystalline,[39] $Na_{0.01}Pb_{0.09}Te$,[18] SnTe,[51] GeTe,[22] and $Bi_{0.05}Ge_{0.95}Te$[65]).

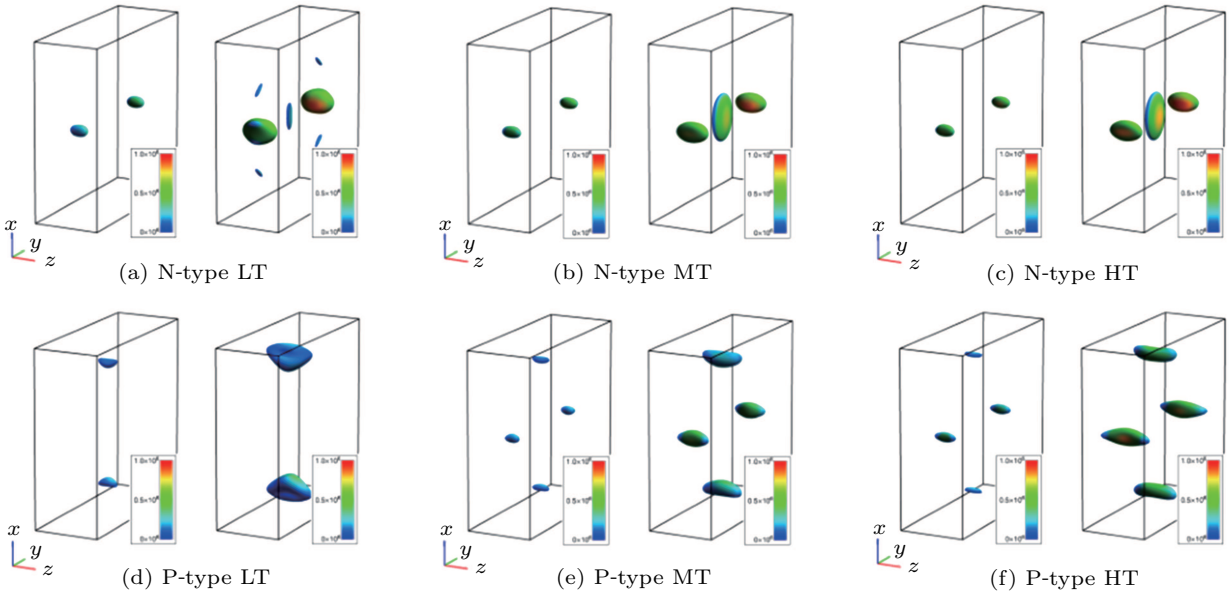


Fig. 8. (color online) Fermi surfaces of the low-temperature (LT) phase, middle-temperature (MT) phase, and high temperature (HT) phase SnSe for [(a)–(c)] N-type and [(d)–(f)] P-type doping for carrier concentrations (in cm^{-3}) of 10^{19} (left) and 10^{20} (right). Electron velocities (in m/s) are represented by a color scale. (Reprinted (figure) from Ref. [71] with permision of Copyright (2015) by American Physical Society).

less than 10^{19} cm^{-3}, the Fermi level makes an ellipsoidal electron pocket with a twofold degeneration, forming a regular and parabolic-like electronic pocket. For the P-type SnSe semiconductor, when the carrier concentration is 10^{20} cm^{-3} for the low-temperature SnSe phase, the Fermi level enters into a hole pocket with nonellipsoidal shape. It was reported that the m^* (effective electron mass) of SnSe is less than the effective hole mass $m^*_N/m^*_P = 1.12 \times 10^{-3}$,[72] suggesting that the electrical conductivity of N-type SnSe would be much higher than that of P-type SnSe.[73] With the principal availability revealed by those preliminary results, it can be expected that N-type group-IV chalcogenide thermoelectrics with high performance in the near future, though there are some technical difficulties, should be implemented.

7. Mechanical and chemical stability

The mechanical and chemical stability is another important issue for the practical device applications of the group- IV chalcogenides thermoelectrics, but few researches have been performed to date. As shown in Table 1, most of those compounds adopt orthohombic structure with space group Pnma, exhibiting a layered structural feature, which means the weak strength and easy decomposition along the crystallographic directions with large periods. Taking SnSe for example, the adjacent layers of SnSe are bound to each other by weak van der Waals and long-range electrostatic attractions.[74,75] This leads to a low friction coefficient of about 0.38 for SnSe,[74] meaning the easy intercrystallite slip decomposition along a specific crystallographic direction.

The Berkovich nano-indentation and Vickers micro-indentation methods can be used to examine the mechanical properties of materials.[53] Figure 9 summarizes the reported Vickers (H_v) micro-hardness values of the popular thermoelectric materials, such as Bi_2Te_3,[76] PbTe,[77] SnTe,[78] PbSe,[79] Cu_2S,[80] Cu_2Se,[80] Bi_2Te_3+$Ge_{0.87}Pb_{0.13}Te$,[81] $Ge_{0.87}Pb_{0.13}Te$,[81] $Ge_{0.9}Sb_{0.1}Te_{0.9}S_{0.05}Se_{0.05}$,[55] $Ge_{0.94}Bi_{0.06}Te$,[82] and GeTe.[82] Here, the GeTe based materials exhibit higher micro-hardness values than others promising chalcogenide thermoelectric materials. The SnTe, PbTe, and PbSe have the same crystal structure, and the micro-hardness value of SnTe is higher than those of PbSe and PbTe. The mechanical performance of the material still needs to be improved for the practical device applications. There are some approaches to improving mechanical properties, such as introducing appropriate defects and dislocations.[83] Grain refinement, nano-inclusion, and texture are also effective ways to enhance the mechanical properties of the materials.[82,84]

In addition, chemical stability of the material is also an improtant factor. Selenide is easily oxidized by long-term exposure to the air,[85] which would harm its thermoelectric performance. It was reported that the surface of polycrystalline SnSe sample is easily oxidized to form tin oxide, leading to much higher thermal conductivity.[86] The low chemical stablilities of Ge- and Si-tellurides would also be detrimental to their applications. Tellurium easily evaporates during heating and tends to form oxides on the surface, which is harmful to their thermoelectric properties.[87] Hence the fabrication and service stablity of the thermoelectric device based on the group-IV chalcogenides, which have not been well explored, need to be studied in depth.

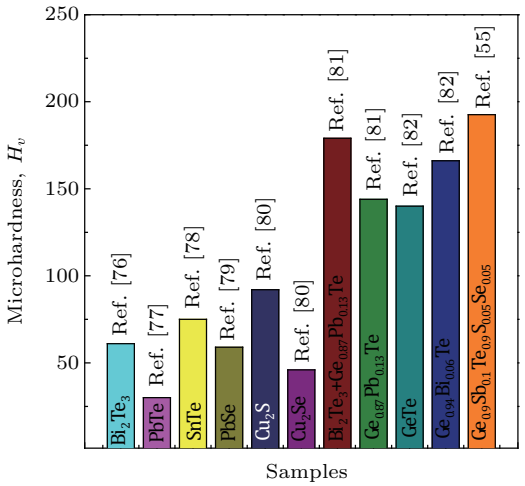


Fig. 9. (color online) Vickers micro-hardness value of group IV–chalcogenides compared with those of other popular thermoelectric materials. (Reprinted (adapted) from Ref. [55] with permission from Copyright (2017) American Chemical Society).

8. Conclusions

Based on the above survey of the recent reports, it is reasonable to conclude that non-Pb based group-IV chalcogenides have emerged as a new promsing thermoelectric material with high performance comparable to (even beyond) that of PbTe besides the advantage of environmental friendship. Most strategies that have been applied to PbTe-based thermoelectrics have proven their availability and effectiveness, which inculde defect engineering, band engineering, nanostructuring, nanoinclusions and modulation doping. During the last several years, notable achievements have been made both experimentally and theoretically, thereby greatly deepening and broadening our knowledge of the thermoelectrics. It could be expected that more exciting and encouraging progress of material research in science and technology would be made in the near future.

References

[1] Minnich A J, Dresselhaus M S, Ren Z F and Chen G 2009 *Energy & Environmental Science* **2** 466

[2] Pan L, Bérardan D, Zhao L D, Barreteau C and Dragoe N 2013 *Appl. Phys. Lett.* **102** 023902

[3] Pei Y L, Tan G J, Feng D, Zheng L, Tan Q, Xie X B, Gong S K, Chen Y, Li J F, He J Q, KanatzidisMG and Zhao L D 2017 *Adv. Energy Mater.* **7** 1601450

[4] Qin P, Qian X, Ge Z H, Zheng L, Feng J, Zhao L D 2017 *Inorg. Chem. Front.* **4** 1192

[5] Zhao H Z, Cao B L, Li S M, Liu N, Shen J W, Li S, Jian J K, Gu L, Pei Y Z, Snyder G J, Ren Z F and Chen X L 2017 *Adv. Energy Mater.* **7** 1700446

[6] Kim Y J, Zhao L D, Kanatzidis M G and Seidman D N 2017 *ACS Appl. Mater. Interfaces* **9** 21791

[7] Jian Z Z, Chen Z W, Li W, Yang J, Zhang W Q and Pei Y Z 2015 *J. Mater. Chem. C* **3** 12410

[8] Li S K, Liu X R, Liu Y D, Liu F S, Luo J and Pan F 2017 *Nano Energy* **39** 297

[9] Tan Q, Wu C F, Sun W and Li J F 2016 *RSC Adv.* **6** 43985

[10] Cao B L, Jian J K, Ge B H, Li S M, Wang H, Liu J and Zhao H Z 2017 *Chin. Phys. B* **26** 017202

[11] Zhao W, Liu Z, Sun Z, Zhang Q, Wei P, Mu X, Zhou H, Li C, Ma S, He D, Ji P, Zhu W, Nie X, Su X, Tang X, Shen B, Dong X, Yang J, Liu Y and Shi J 2017 *Nature* **549** 247

[12] Wang S Y, Sun Y X, Yang J, Duan B, Wu L H, Zhang W Q and Yang J H 2016 *Energy Environ.* **Sci.9** 3436

[13] Ge Z H, Song D, Chong X, Zheng F, Jin L, Qian X, Zheng L, Dunin-Borkowski R E, Qin P, Feng J and Zhao L D 2017 *J. Am. Chem. Soc.* **139** 9714

[14] Mao J, Zhou J W, Zhu H T, Liu Z H, Zhang H, He R, Chen G and Ren Z F 2017 *Chem. Mater.* **29** 867

[15] Hong M, Chasapis T C, Chen Z G, Yang L, Kanatzidis M G, Snyder G J and Zou J 2016 *ACS Nano* **10** 4719

[16] Yamini S A, Mitchell David R G, Gibbs Zachary M, Santos R, Patterson V, Li S, Pei Y Z, Dou S X and Jeffrey Snyder G 2015 *Adv. Energy Mater.* **5** 1501047

[17] Li W, Wu Y X, Lin S Q, Chen Z W, Li J, Zhang X Y, Zheng L L and Pei Y Z 2017 *ACS Energy Lett.* **2** 2349

[18] Chen Z, Jian Z, Li W, Chang Y, Ge B, Hanus R, Yang J, Chen Y, Huang M, Snyder G J and Pei Y Z 2017 *Adv. Mater.* **29** 1606768

[19] Zhao L D, Lo S, Zhang Y, Sun H, Tan G, Uher C, Wolverton C, Dravid V P and Kanatzidis M G 2014 *Nature* **508** 373

[20] Ding G, Gao G and Yao K. 2015 *Sci. Rep.* **5** 9567

[21] Li W, Zheng L, Ge B, Lin S, Zhang X, Chen Z, Chang Y and Pei Y Z 2017 *Adv. Mater.* **29** 1605887

[22] Li J Q, Deng J F, Li S K, Li Y, Liu F S and Ao W Q 2015 *Intermetallics* **56** 63

[23] Wang H, Schechtel E, Pei Y Z, Snyder G and Jeffrey 2013 *Adv. Energy Mater.* **3** 488

[24] Guo R Q, Wang X J, Kuang Y D and Huang B L 2015 *Phys. Rev. B* **92** 115202

[25] Perumal S, Roychowdhury S, Negi D S, Datta R J and Biswas K 2015 *Chem. Mater.* **27** 7171

[26] Hao S Q, Shi F Y, Dravid V P, Kanatzidis M G and Wolverton C 2016 *Chem. Mater.* **28** 3218

[27] Yang J H, Yuan Q H, Deng H X, Wei S H and Yakobson B I. 2017 *The J. Phys. Chem. C* **121** 123

[28] Juneja R, Pandey T and Singh A K 2017 *Chem. Mater.* **29** 3723

[29] Shafique A and Shin Y H 2017 *Sci. Rep.* **7** 506

[30] Brebrick R F and Strauss A J 1963 *Phys. Rev.* **131** 104

[31] Zhao L D, Chang C, Tan G J and Kanatzidis M G 2016 *Energy & Environ. Sci.* **9** 3044

[32] Cao J, Wang Z, Zhan X, Wang Q, Safdar M, Wang Y and He J 2014 *Nanotechnology* **25** 105705

[33] Biljana P and Atanas T 2008 *J. Phys. Chem. C* **112** 3535

[34] Matthew A F, Cody W S, Mark E T and Richard L B 2010 *J. Am. Chem. Soc.* **132** 4060

[35] Liu J, Jian J K, Yu Z Q, Zhang Z H, Cao B L and Du B S 2017 *Crystal Growth & Design* **17** 6163

[36] Butt Faheem K, Mirza M, Cao C B, Idrees F, Tahir M, Safdar M, Ali Z, Tanveer M and Aslam I 2014 *CrystEngComm* **16** 3470

[37] Zhao L D, Tan G J, Hao S Q, He J Q, Pei Y L, Chi H, Wang H, Gong S K, Xu H B, Dravid V P, Uher C, Snyder G J, Wolverton C and Kanatzidis M G 2016 *Science* **351** 141

[38] Peng K L, Lu X, Zhan H, Hui S, Tang X D, Wang G W, Dai J Y, Uher C, Wang G Y and Zhou X Y 2016 *Energy & Environ. Sci.* **9** 454

[39] Sassi S, Candolfi C, Vaney J B, Ohorodniichuk V, Masschelein P, Dauscher A and Lenoir B 2014 *Appl. Phys. Lett.* **104** 212105

[40] Feng D, Ge Z H, Chen Y X, Li J and He J Q 2017 *Nanotechnology* **28** 455707

[41] Guo J, Jian J K, Liu J, Cao B L, Lei R B, Zhang Z H, Song B and Zhao H Z 2017 *Nano Energy* **38** 569

[42] Tang G D, Wei W, Zhang J, Li Y S, Wang X, Xu G Z, Chang C, Wang Z H, Du Y W and Zhao L D 2016 *J. Am. Chem. Soc.* **138** 1647

[43] Lee Y K, Ahn K, Cha J, Zhou C, Kim H S, Choi G, Chae S I, Park J H, Cho S P, Park S H, Sung Y E, Lee W B, Hyeon T and Chung I 2017 *J. Am. Chem. Soc.* **139** 10887

[44] Guo H F, Xin H X, Qin X Y, Zhang J, Li D, Li Y Y, Song C J and Li C 2016 *J. Alloys Compd.* **689** 87

[45] Wei T R, Tan G, Zhang X, Wu C F, Li J F, Dravid V P, Snyder G J and Kanatzidis M G 2016 *J. Am. Chem. Soc.* **138** 8875

[46] Han Y M, Zhao J, Zhou M, Jiang X X, Leng H Q and Li L F 2015 *J. Mater. Chem. A* **3** 4555

[47] Asfandiyar, Wei T R, Li Z, Sun F, Pan Y, Wu C F, Farooq M U, Tang H, Li F, Li B and Li J F 2017 *Sci. Rep.* **7** 43262

[48] Tan Q, Zhao L D, Li J F, Wu C F, Wei T R, Xing Z B and Kanatzidis Mercouri G. 2014 *J. Mater. Chem. A* **2** 17302

[49] Wang H C, Hwang J, Zhang C, Wang T, Su W B, Kim H, Kim J, Zhai J Z, Wang X, Park H J, Kim W and Wang C 2017 *J. Mater. Chem. A* **5** 14165

[50] Zhang X, Wang D Y, Wu H J, Yin M J, Pei Y L, Gong S K, Huang Li, Pennycook S J, He J Q and Zhao L D 2017 *Energy & Environ. Sci.* **10** 2420

[51] Zhang X, Zhou Y M, Pei Y L, Chen Y X, Yuan B F, Zhang S M, Deng Y, Gong S K, He J Q and Zhao L D 2017 *J. Alloys Compd.* **709** 575

[52] Cook B A, Kramer M J, Wei X, Harringa J L and Levin E M 2007 *J. Appl. Phys.* **101** 053715

[53] Perumal S, Roychowdhury S and Biswas K 2016 *J. Mater. Chem. C* **4** 7520

[54] Manisha S, Subhajit R, Jay G, Suresh P and Kanishka B 2017 *Chem. Eur. J.* **23** 7438

[55] Samanta M and Biswas K 2017 *J. Am. Chem. Soc.* **139** 9382

[56] Wu L H, Li X, Wang S Y, Zhang T S, Yang J, Zhang W Q, Chen L D and Yang J H 2017 *NPG Asia Mater.* **9** e343

[57] Li J, Chen Z W, Zhang X Y, Sun Y X, Yang J and Pei Y Z 2017 *NPG Asia Mater.* **9** e353

[58] Ros F D, Dismukes J P and Hockings E F 1960 *Electrical Engineering* **79** 450

[59] Chen Y, Jaworski C M, Gao Y B, Wang H, Zhu T J, Snyder G J, Heremans J P and Zhao X B 2014 *New J. Phys.* **16** 013057

[60] Huang Z, Miller S A, Ge B, Yan M, Anand S, Wu T, Nan P, Zhu Y, ZhuangW, Snyder G J, Jiang P and Bao X 2017 *Angew Chem. Int. Ed. Engl.* **56** 14113

[61] Zhang X Y, Shen J W, Lin S Q, Li J, Chen Z W, Li W and Pei Y Z 2016 *J. Materiomics* **2** 331

[62] Keuleyan S, Wang M, Chung F R, Commons J and Koski K J 2015 *Nano Lett.* **15** 2285

[63] Duong A T, Nguyen V Q, Duvjir G, Duong V T, Kwon S, Song J Y, Lee J K, Lee J E, Park S, Min T, Lee J, Kim J and Cho S 2016 *Nat. Commun.* **7** 13713

[64] Hughes M A, Fedorenko Y, Gholipour B, Yao J, Lee T H, Gwilliam R M, Homewood K P, Hinder S, Hewak D W, Elliott S R and Curry R J 2014 *Nat. Commun.* **5** 5346

[65] Shimano S, Tokura Y and Taguchi Y 2017 *APL Mater.* **5** 056103

[66] Li F, Wang W T, Qiu X C, Zheng Z H, Fan P, Luo J T and Li B 2017 *Inorg. Chem. Front.* **4** 1721

[67] Haldolaarachchige N, Gibson Q, Xie W W, Nielsen M B, Kushwaha S and Cava R J 2016 *Phys. Rev. B* **93** 024520

[68] Li D B, Tan X J, Xu J T, Liu G Q, Jin M, Shao H Z, Huang H J, Zhang J F and Jiang J 2017 *RSC Adv.* **7** 17906

[69] Wang X, Xu J, Liu G Q, Fu Y J, Liu Z, Tan X J, Shao H Z, Jiang H C, Tan T Y and Jiang J 2016 *Appl. Phys. Lett.* **108** 083902

[70] Pei Y Z, Gibbs Z M, Gloskovskii A, Balke B, Zeier W G and Snyder G Jeffrey 2014 *Adv. Energy Mater.* **4** 1400486

[71] Kutorasinski K, Wiendlocha B, Kaprzyk S and Tobola J 2015 *Phys. Rev. B* **91** 205201
[72] Nassary M M 2009 *Turk. J. Phys.* **33** 201
[73] Yang J M, Zhang J B, Yang G, Wang C and Wang Y X 2015 *J. Alloys Compd.* **644** 615
[74] Erdemir A 1994 *Tribology Transactions* **37** 471
[75] Zallen R and Slade M 1974 *Phys. Rev. B* **9** 1627
[76] Zhao L D, Zhang P B, Li J F, Zhou M, Liu W S and Liu J 2008 *J. Alloys Compd.* **455** 259
[77] Gelbstein Y, Gotesman G, Lishzinker Y, Dashevsky Z and Dariel M P 2008 *Scr. Mater.* **58** 251
[78] Cui J L, Qian X and Zhao X B 2003 *J. Alloys Compd.* **358** 228
[79] Darrow W B W M S and Roy R 1969 *J. Mater. Sci.* **313**
[80] Zhao L, Wang X, Fei F Y, Wang J, Cheng Z, Dou S, Wanga J and Snyder G J 2015 *J. Mater. Chem. A* **3** 9432
[81] Davidow J and Gelbstein Y 2013 *J. Electron. Mater.* **42** 7
[82] Perumal S, Roychowdhury S and Biswas K 2016 *Inorg. Chem. Front.* **3** 125
[83] Li G, Gadelrab K R, Souier T, Potapov P L, Chen G and Chiesa M 2012 *Nanotechnology* **23** 065703
[84] Fanciulli C, Coduri M, Boldrini S, Abedi H, Tomasi C, Famengo A, Ferrario A, Fabrizio M and Passaretti F 2017 *J. Nanosci. Nanotechnol.* **17** 1571
[85] Kergommeaux A D, Faure-Vincent J, Pron A, Bettignies R, Malaman B and Reiss P 2012 *J. Am. Chem. Soc.* **134** 11659
[86] Li Y, He B, Heremans J P and Zhao J C 2016 *J. Alloys Compd.* **669** 224
[87] Keuleyan S, Wang M J, Chung F R, Commons J and Koski K J 2015 *Nano Lett.* **15** 2258